

Growth Study of Cuprate Thin Films by PLD

Department of Advanced Materials Science, 086007, Yuichi Ota

Advisor: Prof. Harold Y. Hwang

Keywords: PLD, Cuprate, High- T_c superconductor, Ozone

Introduction

Transition metal oxide thin films have been attracting many researchers. One of the most striking phenomena can be seen in the heterostructures of high- T_c superconductors. In superlattice [1], multilayer [2], and strongly-oxidized and -strained thin films [3], unconventional superconductivity which cannot be realized in bulk has been observed. For fabricating such thin films, pulsed laser deposition (PLD) is suitable because it is a relatively simple and flexible technique for the deposition of high-quality films from multi-component materials. It is, however, well known that precise control of the growth parameters is required. As suggested in the growth of titanate and manganite [4,5], the optimization of the laser conditions is particularly important. In addition, it was reported that the strong oxidization by ozone dramatically enhanced the superconducting properties of cuprate thin films [3]. In this thesis, we describe the optimization of the laser condition for the growth of $\text{La}_{2-x}\text{Sr}_x\text{CuO}_4$ thin films. We also report the achievement of utilizing ozone which brings about the enhancement of superconducting properties.

Experimental

$\text{La}_{1.85}\text{Sr}_{0.15}\text{CuO}_4$ films were grown on LaSrAlO_4 (001) substrates by PLD using a KrF excimer laser ($\lambda = 248$ nm) at the temperature of 780 °C and the oxygen partial pressure of 1.0×10^{-2} Torr. All film thicknesses are set constant at 1000 Å. The laser energy and the cooling conditions were varied depending on the purposes. The surface morphology was measured by atomic force microscopy (AFM), and the c -axis length and FWHM of the film (004) peak were characterized by 2θ - ω x-ray diffraction (XRD). The film thickness was *ex-situ* confirmed with a stylus profilometer. For four-probe resistivity measurements, gold contacts were attached onto the film which was cut into a size of 1.0×5.0 mm². For inductively coupled plasma (ICP) measurements, we fabricated the films on B-doped Si substrates at room temperature. During the deposition, the oxygen pressure and the laser conditions were changed depending on the purposes.

Spot size variation

We fabricated four $\text{La}_{1.85}\text{Sr}_{0.15}\text{CuO}_4$ films with different spot sizes of area 3.5, 5.0, 8.0, and 12.0 mm².

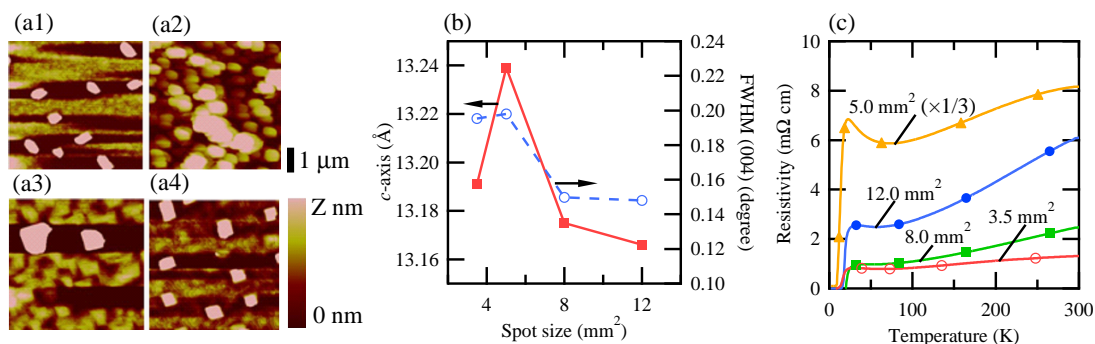


Figure 1: (a) The surface morphology of the films with thickness 1000 Å, measured by AFM. Laser spot sizes and vertical scales Z are (a1) 3.5 mm² and $Z = 5.0$, (a2) 5.0 mm² and $Z = 5.0$, (a3) 8.0 mm² and $Z = 30$, and (a4) 12.0 mm² and $Z = 5.0$. (b) c -axis length and FWHM of the (004) peak are plotted as a function of spot size. The solid lines indicate c -axis, and the dashed lines FWHM. (c) Resistivity as a function of temperature. Open circles, closed triangles, closed squares, and closed circles correspond to the samples grown with spot sizes of 3.5, 5.0, 8.0, and 12.0 mm², respectively. The vertical scale for the 5.0 mm² sample is reduced by a factor of three for clarity.

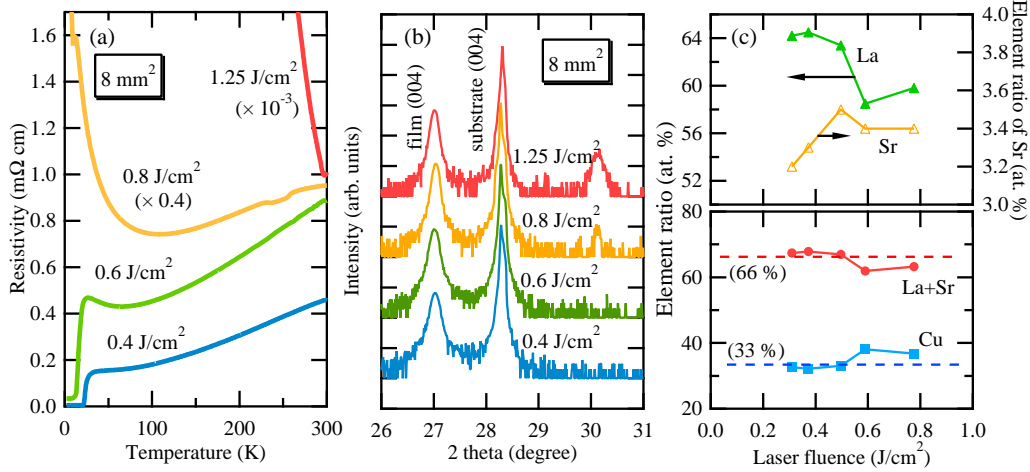


Figure 2: (a) Resistivity of $\text{La}_{2-x}\text{Sr}_x\text{CuO}_4$ thin films as a function of temperature. All films were grown on LaSrAlO_4 (001) substrates using the $\text{La}_{1.85}\text{Sr}_{0.15}\text{CuO}_4$ target. The vertical scale for the 1.25 and 0.8 J/cm^2 samples are reduced by a factor of 10^{-3} and 0.4 for clarity. (b) 2θ - ω scans around the film (004) peak. The satellite peaks which can be seen in the 1.25 and 0.8 J/cm^2 samples are the impurity peaks. (c) Element ratio of the samples with different laser fluence measured by ICP. The spot size was set constant at 12 mm^2 . Closed triangles, opened triangles, closed circles and closed squares represent the ratio of La, Sr, (La+Sr) and Cu, respectively. The dashed lines are the stoichiometric values of (La+Sr) and Cu.

After the depositions, the samples were cooled down at the rate of $-15\text{ }^\circ\text{C}/\text{min}$. without changing oxygen pressure from the deposition pressure. As shown in Figs. 1 (a1) - (a4), there are clearly two types of surfaces. One type is covered with rectangular precipitates on top of screwed terraces, as observed in Figs. 1 (a1), (a3), and (a4). The other is a surface with many circular islands, as seen in Fig. 1 (a2). In comparison with XRD analysis shown in Fig. 1 (b), we can recognize a trade-off. The former have shorter c -axis and high crystallinity and the latter have longer c -axis and low crystallinity. From this trend, we see that high crystallinity is achieved at the cost of high density of circular precipitates, and the origin of the longer c -axis with low density of rectangular precipitates is due to some repulsive disorder inside the film. As expected, the trend of resistivity as shown in Fig. 1 (c) follows the changes of the morphology and the crystallinity. The former three samples show a sharp superconducting transition, whereas the latter one has large resistivity, an upturn just before the onset of superconductivity, and a broad transition. The fact that Cooper pairs are easily broken by potentials arising from impurities and grain boundaries in the CuO_2 plane supports this correlation between the morphology, the crystallinity, and the superconducting properties.

Laser fluence variation

Next, we fabricated $\text{La}_{1.85}\text{Sr}_{0.15}\text{CuO}_4$ films by changing the laser fluence at the spot sizes of area 2.5, 8.0 and 12.0 mm^2 . In this series of samples, we cooled down the temperature at the rate of $-10\text{ }^\circ\text{C}/\text{min}$. During the cooling, we temporarily stopped and kept at the temperature of $400\text{ }^\circ\text{C}$ for 30 min. to conduct *in-situ* annealing. As a representative example, here we will take the series of samples made with the spot size of area 8.0 mm^2 . As shown in Fig. 2 (a), the film was insulating at the high laser fluence, whereas superconducting at the low laser fluence. The resistivity results resemble the systematic trend of Sr doping concentration gradually changing from the underdoped regime to the optimal doped regime as the laser fluence decreases. In Fig. 2 (b), we can see the impurity peak around $2\theta = 30^\circ$ of the samples with high laser fluence, which may originate from the La_2O_3 (101) peak. Intensity of the impurity peak decreases as the laser fluence decreases, disappearing below $0.6\text{ J}/\text{cm}^2$. From these results, we can expect that the amount of La decreases and that of Sr increases as the laser fluence decreases. On the other hand, from the result of ICP as shown in Fig. 2 (c), the amounts of both elements change oppositely to our expectation. This possibly indicates that the element composition in the final film which detected resistivity and XRD is different from that which is supplied from the target to the substrate. Considering the fact that all films

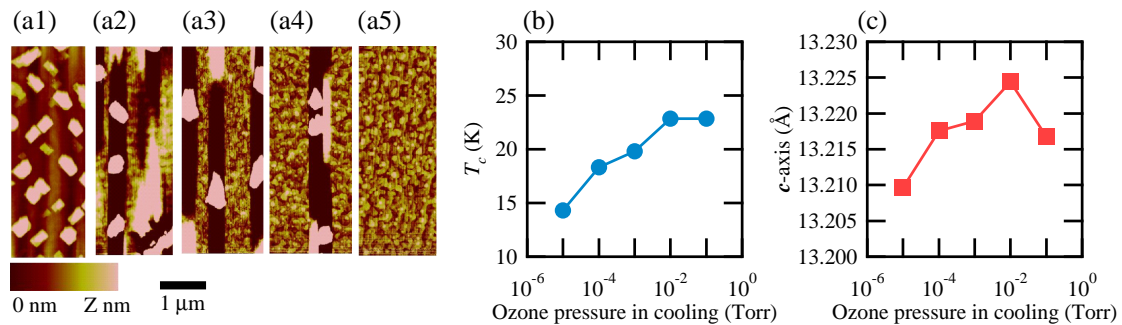


Figure 3: (a) The surface morphology of the films with different cooling pressure of ozone. The ozone pressures and the vertical scales are (a1) 10^{-5} Torr and $Z = 30$, (a2) 10^{-4} Torr and $Z = 2.0$, (a3) 10^{-3} Torr and $Z = 2.0$, (a4) 10^{-2} Torr and $Z = 2.0$, and (a5) 10^{-1} Torr and $Z = 2.0$. (b) and (c) are T_c and c -axis length as a function of the laser fluence, respectively.

have precipitates on their surfaces, the crystallization process of crystalline film and the generation process of precipitates can be concluded as key issues to understand this results.

Ozone cooling

We utilized ozone in the cooling procedure. After fabricating five same samples in the laser conditions of 0.3 J/cm^2 with the spot size of area 12 mm^2 , we cooled them down in ozone atmosphere. The cooling rate and the *in-situ* annealing conditions were the same. As shown in Fig. 3 (a), the number of precipitates on the surfaces gradually decreases as the ozone pressure increases. Coincidentally, T_c increases and c -axis expands. The higher pressure ozone is obviously suitable for making high-quality superconducting films. Taking into account that the films are stoichiometric in this laser condition as shown in Fig. 2 (c), the precipitates seem to be integrated into the inside of the films assisted by the oxidization power of ozone. We not only reproduced the enhancement of superconducting properties as suggested [3], but also discovered that ozone strongly affects the generation process of precipitates in the cooling procedure.

Conclusion

In conclusion, we fabricated $\text{La}_{1.85}\text{Sr}_{0.15}\text{CuO}_4$ thin films by PLD with changing the different laser conditions and the cooling procedure, and then studied the correlation between morphology, crystallinity, and superconducting behavior. As a result, we found that high crystallinity samples with sharp superconducting transition was obtained at the cost of precipitates on the film surface. As for the laser conditions, we found that lower laser fluence was optimal to make $\text{La}_{1.85}\text{Sr}_{0.15}\text{CuO}_4$ thin films. In addition, we found that ozone cooling dramatically enhanced the quality of samples. Throughout this study, we achieved to optimize the growth conditions of cuprate thin films by PLD. Based on these results/findings, we tried making a photoactive device utilizing the interface $\text{La}_{1.85}\text{Sr}_{0.15}\text{CuO}_4/\text{SrTiO}_3$ [6]. By further improvement for making ultra-thin films, we can expect to access the fundamental mechanism of high- T_c superconductors and to enhance the quality of the photoactive device.

References

- [1] D. P. Norton *et al.*, Science **265**, 2074 (1994).
- [2] A. Gozar *et al.*, Nature **455**, 782 (2008).
- [3] H. Sato *et al.*, Phys. Rev. B **61**, 12447 (2000).
- [4] T. Ohnishi *et al.*, Appl. Phys. Lett. **87**, 241919 (2005).
- [5] J. H. Song *et al.*, Adv. Mater. **20**, 2528 (2008).
- [6] Z. Hiroi *et al.*, Kotai Butsuri **39**, 211 (2003).

Presentations and publication

1. Y. Ota, Y. Kozuka, J. H. Song, Y. Hikita, and H. Y. Hwang, JSAP 69th Spring meeting, 29a-L-10 (2008) (oral).
2. Y. Ota, Y. Kozuka, Y. Hikita, and H. Y. Hwang, JSAP 55th Autumn meeting, 2p-J-9 (2008) (oral).
3. Y. Ota, Y. Kozuka, J. H. Song, Y. Hikita, and H. Y. Hwang, ISAQM 2008 and The 7th APW, PSA-20 (2008) (poster).
4. Y. Ota, Y. Kozuka, J. H. Song, Y. Hikita, and H. Y. Hwang, 2009 MRS Spring meeting, (2009) (poster).
5. Y. Ota, Y. Kozuka, Y. Hikita, and H. Y. Hwang (paper, in preparation).